

# High-frequency domain wall excitations in magnetic garnet films with in-plane magnetization

V. T. Synogach

*Institute for Solid State Physics, Russian Academy of Sciences, Chernogolovka, Moscow district, 142432 Russia*

H. Dötsch

*University of Osnabrück, 49069 Osnabrück, Germany*

(Received 6 February 1996; revised manuscript received 13 May 1996)

Magnetic garnet films of compositions  $(\text{YBi})_3\text{Fe}_5\text{O}_{12}$  and  $(\text{LuBi})_3\text{Fe}_5\text{O}_{12}$  are grown by liquid-phase epitaxy on [110]- and [100]-oriented substrates of gadolinium gallium garnet, respectively. All films have in-plane magnetization.  $180^\circ$  and  $90^\circ$  domain walls in these films are studied by microwave technique. In addition to the known low-frequency mode of wall translation new multiple resonant modes of both  $90^\circ$  and  $180^\circ$  domain walls with very small linewidth (4.2 MHz) are observed at frequencies near 1 GHz. Resonances are effectively excited by an rf magnetic field which is parallel or perpendicular to the wall plane. Resonance frequencies are shown to have nonlinear dispersion dependence on the mode number: they decrease with increasing in-plane magnetic field normal to the wall plane. [S0163-1829(96)03245-6]

## I. INTRODUCTION

Magnetic garnet films possessing in-plane magnetization and small magnetic anisotropy represent an interesting class of materials both for basic and applied research. In comparison to well studied garnet films with perpendicular magnetization they are supposed to have additional types of elementary excitations related to domains, domain walls, and Bloch lines. They may reveal more complicated nonlinear and chaotic behavior. The combination of well controllable magnetic and optical properties make such crystals attractive for applications in optical communications systems. Static and dynamic properties of magnetic domains and domain walls of in-plane magnetized garnet films are not so intensively studied in the past as films with large perpendicular anisotropy (bubble films<sup>1</sup>). The theory of domain-wall excitations was developed for the case of bulk low-anisotropy uniaxial ferromagnets<sup>2</sup> and for the case of crystals with cubic magnetic anisotropy and an additional small uniaxial anisotropy (as in pure yttrium iron garnet, YIG).<sup>3</sup> In addition to a well-known low-frequency branch of wall translations, the existence of high-frequency branches in the spectrum of the wall excitations is predicted. These branches are of magnetostatic origin,<sup>2</sup> or are related to the wall structure.<sup>3</sup> Up to now only low-frequency  $180^\circ$  domain-wall excitations were studied experimentally in YIG.<sup>4,5</sup> In this paper experimental results on high-frequency resonant modes of  $90^\circ$  and  $180^\circ$  domain walls in low-anisotropy [110]- and [100]-oriented bismuth-substituted garnet films with in-plane magnetization are presented.

## II. SAMPLES AND EXPERIMENTAL TECHNIQUE

Bi-substituted yttrium and lutetium iron garnet films (Bi:YIG and Bi:LIG) are grown by liquid-phase epitaxy on [110]- and [100]-oriented substrates of gadolinium gallium garnet. Compositions and parameters of investigated samples are listed in Table I. Saturation magnetization  $M_s$  is supposed to be equal to that of pure YIG:  $M_s = 1.49 \times 10^5$  A/m.

Constants of cubic, uniaxial, and orthorhombic anisotropies  $K_1$ ,  $K_u$ ,  $K_i$ , and the gyromagnetic ratio are determined from ferromagnetic resonance (FMR) measurements, damping parameter  $\alpha$  from the FMR linewidth. Magnetization in the film plane was realized due to the appropriate choice of material parameters.

To determine regions in the space of anisotropy parameters  $(K_1, K_u, K_i)$  corresponding to in-plane magnetization we calculate the equilibrium position of the magnetization of a homogeneously magnetized film by minimizing the free energy. The coordinate system for the case of [110]-oriented films is shown in Fig. 1. An appropriate system for the case of [100]-oriented films coincides with the usual cubic one, i.e.,  $x$ ,  $y$ , and  $z$  axes are [100], [010], and [001] directions, respectively. Magnetization vector  $\mathbf{M}$  is defined by the polar angle  $\theta$  and the azimuth  $\varphi$ :

$$\mathbf{M} = M_s(\sin\theta \cos\varphi, \sin\theta \sin\varphi, \cos\theta). \quad (1)$$

The free-energy density

$$F = F_u + F_i + F_c + F_d \quad (2)$$

consists of uniaxial anisotropy energy:

$$F_u = K_u \sin^2\theta, \quad (3)$$

TABLE I. Material parameters of investigated garnet films.

Sample No. <sup>a</sup>	1	2	3	Unit
Orientation	[110]	[110]	[100]	
$d$	3.9	5.4	2.7	$\mu\text{m}$
$K_1$	-0.60	-0.61	-0.72	$\text{kJ/m}^3$
$K_u$	-2.60	-1.90	-0.93	$\text{kJ/m}^3$
$K_i$	0.54	0.69		$\text{kJ/m}^3$
$10^3\alpha$	0.9	2.0	1.2	
$\gamma/2\pi$	28.2	28.2	28.2	MHz/mT

<sup>a</sup>Samples 1, 2 are of composition  $\text{Y}_{2.6}\text{Bi}_{0.4}\text{Fe}_3\text{O}_{12}$  and sample 3 is  $\text{La}_{2.2}\text{Bi}_{0.8}\text{Fe}_3\text{O}_{12}$ .

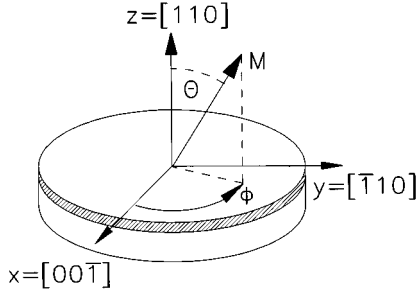


FIG. 1. Coordinate system used to describe [110]-oriented garnet films.

cubic anisotropy energy for [110]-oriented films:

$$F_c = \frac{K_1}{1} \sin^2 \theta (2 \cos^2 \varphi - 3 \sin^2 \theta \cos^4 \varphi - 4 \cos^2 \theta \sin^2 \varphi) \quad (4)$$

and for [100] films:

$$F_c = \frac{K_1}{1} (\sin^2 2\theta + \sin^4 \theta \sin^2 2\varphi) \quad (5)$$

and demagnetizing energy:

$$F_d = \frac{\mu_0 M_s^2}{2} \cos^2 \theta. \quad (6)$$

Orthorhombic anisotropy energy vanishes for [100] films, while for [110]-oriented ones it reads

$$F_i = K_i \sin^2 \theta \sin^2 \varphi. \quad (7)$$

Denoting derivatives by the respective subscripts the energy minimum is derived from equations,

$$F_{\theta} = F_{\varphi} = 0, \quad (8)$$

and the following conditions have to be satisfied:

$$D = F_{\theta\theta} F_{\varphi\varphi} - F_{\theta\varphi}^2 > 0, \quad F_{\theta\theta} > 0. \quad (9)$$

Solving Eqs. (1)–(9) in terms of so-called  $Q$  factors  $Q = 2K_u/\mu_0 M_s^2$ ,  $Q_i = 2K_i/\mu_0 M_s^2$ ,  $Q_1 = 2K_1/\mu_0 M_s^2$ , one obtains for [100]-oriented films:

$$\theta = \frac{\pi}{2}, \quad \varphi = 0, \frac{\pi}{2}, \pi, \frac{3\pi}{2}, \quad (10)$$

$$Q_1 > 0, \quad 1 - Q > -Q_1,$$

$$\theta = \frac{\pi}{2}, \quad \varphi = \frac{\pi}{4}, \frac{3\pi}{4},$$

$$Q_1 < 0, \quad 1 - Q > \frac{-Q_1}{2}, \quad (11)$$

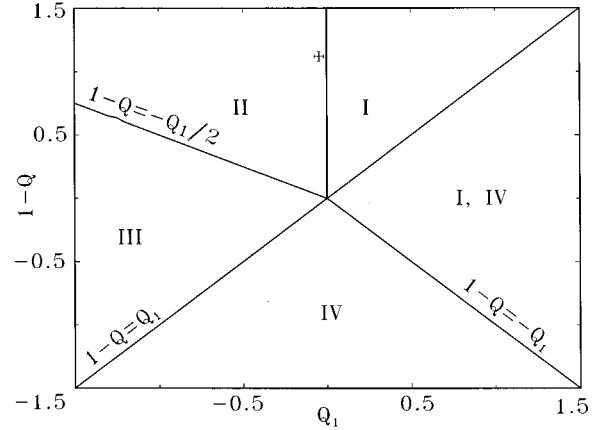


FIG. 2. Plane of cubic and uniaxial anisotropy parameters ( $Q_1$ ,  $1-Q$ ) divided into regions with different equilibrium directions of magnetization for [100]-oriented films. Regions I, II, III, and IV correspond to inequalities (10), (11), (12), and (13), respectively. Investigated  $\text{Lu}_{2.2}\text{Bi}_{0.8}\text{Fe}_5\text{O}_{12}$  film (sample 3) is pointed out by + symbol.

$$\theta = \pm \theta_0, \quad \cos 2\theta_0 = \frac{4(1-Q)}{3Q_1} - \frac{1}{3}, \quad \varphi = \frac{\pi}{4}, \frac{3\pi}{4},$$

$$Q_1 < 0, \quad Q_1 < 1 - Q < \frac{-Q_1}{2}, \quad (12)$$

$$\theta = 0, \quad 1 - Q < Q_1. \quad (13)$$

Note that for the last case Eq. (13)  $D=0$  because  $F_{\theta\varphi} = F_{\varphi\theta} = 0$ . In the neighborhood of the critical point  $\theta=0$  the function  $F(\theta, \varphi) \sim (1/2)F_{\theta\theta}\theta^2$  and instead of Eq. (9) the only condition  $F_{\theta\theta} > 0$  has to be satisfied. Inequalities (10), (11), and (12) correspond to the existence of an in-plane component of the magnetization. They are graphically presented in Fig. 2 in the  $(1-Q, Q_1)$  plane as regions I, II, and III, respectively. In region III the magnetization is tilted by the angle  $\theta_0$  with respect to the film normal. Inequality (13) corresponds to the case of the well studied films with perpendicular magnetization. It is marked as region IV in Fig. 2. In the overlap of regions I and IV two minima of the free energy coexist. Our investigated sample 3 (Bi:LIG) shown by a cross in Fig. 2 supports domains with in-plane magnetization parallel to the [011] and [011] directions (region II in Fig. 2).

Similar solutions for [110]-oriented films are of the form

$$\theta = 0, \quad Q_i < \frac{3}{2} Q_1, \quad 1 - Q < Q_i - Q_1, \quad (14)$$

$$\theta = 0, \quad Q_i > \frac{3}{2} Q_1, \quad 1 - Q < \frac{Q_1}{2}, \quad (15)$$

$$\theta = \frac{\pi}{2}, \quad \varphi = 0, \pi, \quad Q_i > -Q_1, \quad 1 - Q > -Q_1, \quad (16)$$

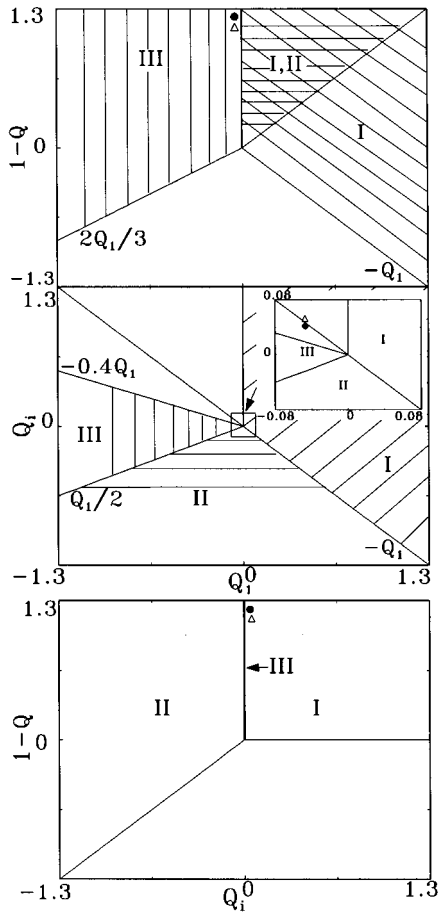


FIG. 3. Plane sections in the space of anisotropy parameters divided into regions with different equilibrium directions of magnetization for [110]-oriented films. Plane of cubic and uniaxial anisotropy parameters  $(Q_1, 1-Q)$  is the top plot, cubic and orthorhombic anisotropy parameters  $(Q_1, Q_i)$  is the central and orthorhombic, and uniaxial anisotropy parameters  $(Q_i, 1-Q)$  plane is the bottom plot. Regions I, II, and III correspond to inequalities (16), (17), and (18), respectively. In the bottom plot region III coincides with the positive  $(1-Q)$  half-axis. Investigated films are pointed out by ● (sample 1) and △ (sample 2).

$$\theta = \frac{\pi}{2}, \quad \varphi = \frac{\pi}{2}, \frac{3}{2}\pi, \quad Q_i < \frac{Q_1}{2}, \quad 1-Q > Q_i + Q_1, \quad (17)$$

$$\theta = \frac{\pi}{2}, \quad \varphi = \pm \varphi_0, \quad \cos 2\varphi_0 = -\frac{1}{3} - \frac{4Q_i}{3Q_1},$$

$$Q_1 < 0, \quad \frac{Q_1}{2} < Q_i < -Q_1, \quad 1-Q > \frac{2}{3}Q_1 + \frac{5}{3}Q_i. \quad (18)$$

The space of anisotropy parameters is now three dimensional. For graphical visualization projections onto the three orthogonal planes  $(Q_1, 1-Q)$ ,  $(Q_1, Q_i)$ , and  $(Q_i, 1-Q)$  through the origin are used (see Fig. 3). To keep Fig. 3 clear, only the regions of in-plane magnetization are shown. Regions I, II, and III correspond to solutions (16), (17), and (18), respectively. Two investigated samples of Bi:YIG have in-plane magnetization directed along the [001] axis (sample

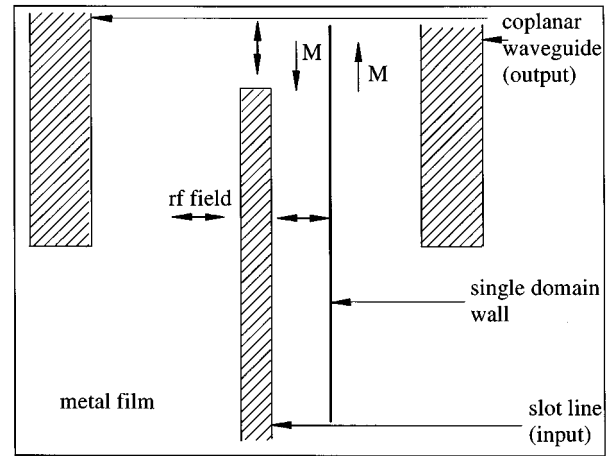


FIG. 4. Sketch of the planar microwave antenna used to excite and detect domain wall resonances.

2) or at the angle  $\phi_0 \sim 18^\circ$  (sample 1). Appropriate points in the  $Q_1 Q_i Q_i$  space are located in region I (△, sample 2) and region III (●, sample 1). In the projection planes of Fig. 3, however, they appear in other regions.

In a transmission polarizing microscope domain walls can be visualized due to the Faraday effect. Therefore, the walls possess a large magnetization component perpendicular to the film plane which is characteristic for Bloch walls. In samples 2 and 3 Bloch lines dividing the wall into bright and dark subdomains are observed.

A planar excitation-detection structure—slot line and coplanar waveguide—is used to study the domain wall response to the high-frequency magnetic field<sup>6</sup> (see Fig. 4). The short-circuited slot line is used as rf input and the short-circuited coplanar waveguide as monitor output. By shifting a sample across the antenna structure a single domain wall is placed between the coplanar waveguide branch and the slot line parallel to the slot. Another way for wall positioning is to use a dc induction parallel to the magnetization in the domains which shifts the wall. After positioning of the wall this induction is switched off. The main exciting rf magnetic fields are indicated by double arrows. They are parallel to the plane of the film which lies on top of the excitation structure.

### III. DOMAIN WALL RESONANCES IN [110]-ORIENTED GARNET FILMS

Single  $180^\circ$  straight plane domain walls are observed in [110]-oriented garnet films. Only near the edge of the sample strongly curved walls are seen (sample 1). Closure domains in the form of splitting wedges are also observed (sample 2). The thickness of the wall image in a microscope is  $\leq 0.5 \mu\text{m}$ , which is the resolution limit of the microscope. We have calculated the static structure of a simple Bloch wall using the technique of Ref. 7:

$$\cot \psi = q \sinh \frac{x}{\Delta}, \quad (19)$$

where the  $x$  axis is normal to the wall plane and coincides with the [110] direction,  $\psi$  is the angle between the magne-

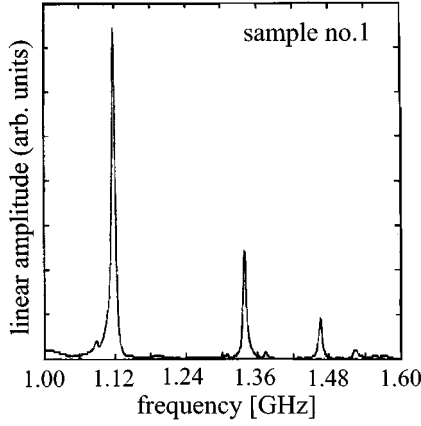


FIG. 5. Broad-band frequency sweep of a single domain wall response in [110]-oriented Bi-garnet film.

tization vector and the  $[00\bar{1}]$  direction, and  $A$  is the exchange constant. The parameters  $q$  and  $\Delta$  are given by

$$q^2 = \frac{K_1 - 4K_u}{4(K_1 - K_u)}, \quad \Delta^2 = \frac{A}{K_1 - k_u}. \quad (20)$$

A large wall thickness occurs in the films if  $K_1 \approx K_u$ . The calculated value of the wall thickness parameter is  $\Delta \approx 0.06 \mu\text{m}$  for sample 2 (for  $A$  an estimated value of  $4 \times 10^{-12} \text{ J/m}$  is used). Notice that the exact solution for the pure Bloch wall with the above structure of Eq. (19) exists only when the magnetization vector in domains is parallel to the  $[00\bar{1}]$  direction. This requirement is fulfilled for sample 2, but not for sample 1.

The measured frequency response of a single domain wall shows a set of sharp resonances (Fig. 5). When the wall is removed out of the excitation region only resonant modes related to the FMR or domain modes are observed at higher frequencies. The linewidth of observed wall resonances is very small. The lowest measured value is 4.2 MHz (see Fig. 6). Rotating the sample so that the wall is perpendicular to the slot line we observe the same resonances. In this case the main exciting field is parallel to the wall plane.

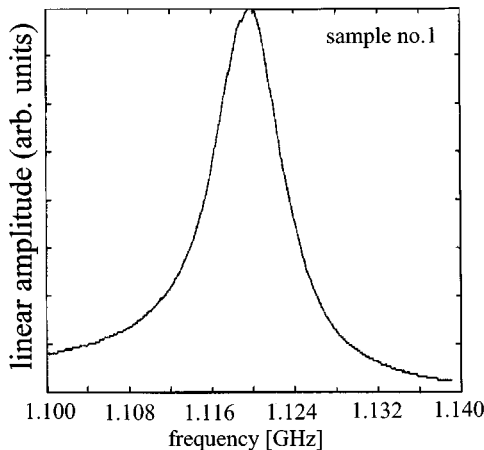


FIG. 6. Narrow-band frequency sweep of the first resonant mode of Fig. 5.

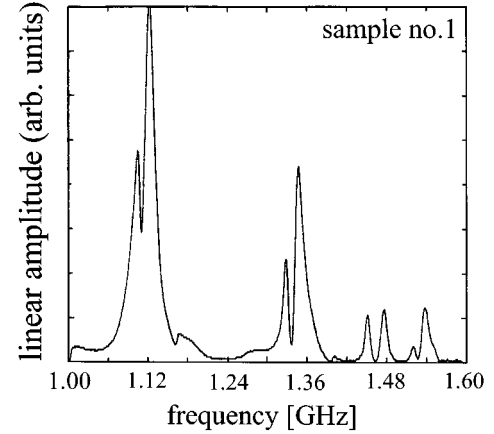


FIG. 7. Frequency response of two coupled domain walls in [110]-oriented Bi-garnet film (sample 1). The distance between the walls is estimated to be about  $1 \mu\text{m}$ .

In addition, the resonance frequencies are independent of the location of the domain wall within the sample. Furthermore, they do not depend on the geometric form of the sample.

In a further experiment two domain walls are placed in the same exciting rf field simultaneously (parallel to the slot line, between the slot and the right branch of the coplanar waveguide). The measured signal is found to be approximately twice as large as that for a single wall. If a dc induction is applied in the film plane parallel to domain magnetization the distance between the two walls decreases and a strong coupling occurs. Each domain wall resonance is split into two coupled resonance modes (see Fig. 7).

Another situation is realized by placing two walls parallel to the slot line on each side of the slot simultaneously. The same resonance modes are observed in this case but the signal amplitude is much smaller than that for the case of a single domain wall.

If a static induction  $\mathbf{B}_0$  is applied perpendicular to the wall plane the resonance frequencies decrease with increasing  $\mathbf{B}_0$  (see Fig. 8). This behavior is similar to that observed for the low-frequency wall resonances in YIG.<sup>8</sup>

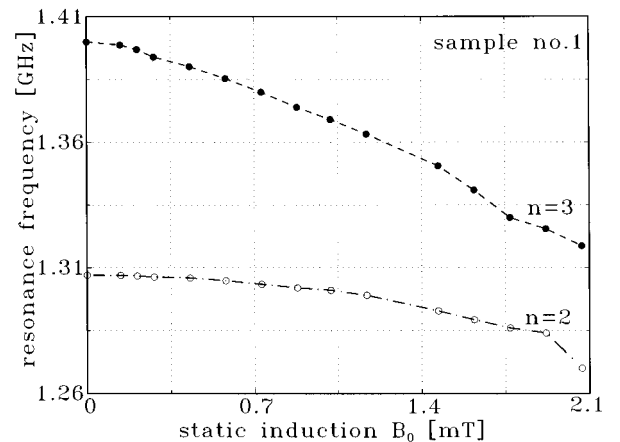


FIG. 8. Dependence of domain wall resonance frequency on dc induction  $\mathbf{B}_0$  applied normal to the wall plane for the second ( $n=2$ ) and third ( $n=3$ ) resonance mode.

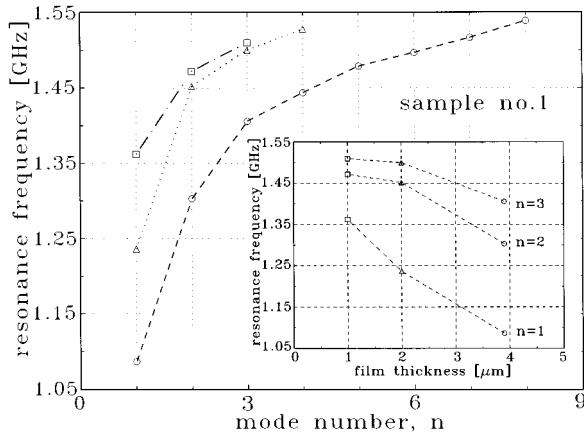


FIG. 9. Plot of domain wall resonance frequency vs mode number  $n$  at different thicknesses  $d$  of the same garnet film (sample 1):  $d=3.9 \mu\text{m}$  ( $\circ$ ),  $2 \mu\text{m}$  ( $\triangle$ ),  $1 \mu\text{m}$  ( $\square$ ).

The observed multiple resonances are assumed to be due to the excitation of standing waves at frequencies  $\omega_n$  defined by the film thickness  $d$  and the dispersion law:  $\omega_n = \omega_n(k_n) = \omega(\pi n/d)$ , where  $n=0,1,2,3,\dots$  is the integer mode number. It is not yet clear, whether mode counting should be started with  $n=0$  or  $n=1$ : this depends on the pinning conditions at the film surfaces which are unknown. In the following we number the modes starting with  $n=1$ , keeping in mind that the first of the observed resonances may be actually related to the uniform zero mode. It is further assumed that both even and odd modes are observed equally well because exciting and detected fields of the used antenna structure are strongly inhomogeneous. A further discussion of this point follows below. The standing wave assumption is supported by experiments to determine the dependence of resonance frequencies on the film thickness  $d$ . These measurements are made after subsequent film etching in phosphoric acid. The increase of resonance frequencies with decreasing  $d$  is revealed in Fig. 9. In the same figure the nonlinear dispersion dependence of the wall resonance frequencies on mode number is presented.

Besides the high-frequency modes also the known low-frequency modes of the same single domain wall are observed in our experiments. Appropriate dispersion dependence of the resonance frequency vs mode number is shown in Fig. 10 for sample 2. Linear dispersion of the low-frequency wall vibrations is clearly seen at low mode numbers similar to the previous observations of single wall resonances related to the flexural wall vibrations in YIG.<sup>4</sup>

Existing theories for low-anisotropy ferromagnets<sup>2,3,9</sup> predict several branches of the domain wall excitation spectrum. In the pure uniaxial ferromagnet there exist a low-frequency branch (Goldstone mode) and the higher-frequency Gilinskii branch.

The Goldstone mode corresponds to pure wall translations or flexural wall vibrations. It is effectively excited by rf fields parallel to the magnetization in the domains. The mode possesses an asymmetric dispersion law:  $\omega(k) \neq \omega(-k)$ .<sup>2,3</sup> Due to this asymmetry both even and odd modes are strongly excited (see the discussion of the asymmetry for the case of

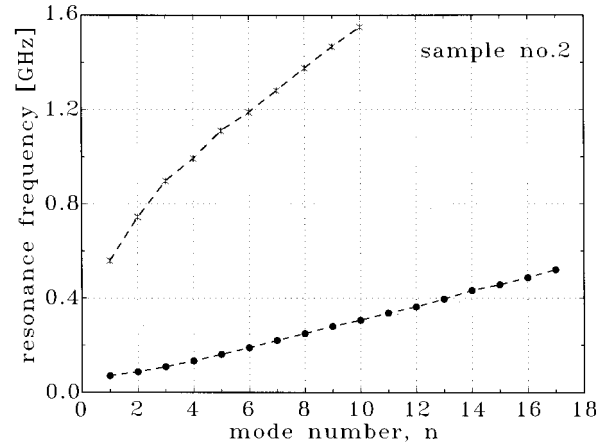


FIG. 10. Plot of resonance frequency vs mode number  $n$  of high- and low-frequency modes ( $*$  and  $\bullet$ , respectively) of the wall vibrations in a  $[110]$ -oriented film.

standing waves in Ref. 4). The pure Goldstone mode has zero frequency at  $k=0$ . However, due to dipole forces induced by sample edges a finite restoring force  $\kappa$  is created. Thus the frequency of the pure translational mode is  $\omega_0 = \omega(k=0) = (\kappa/m)^{1/2}$  ( $m$  is the effective mass of the wall). On the other hand, the higher-order or flexural modes are mainly determined by the material parameters saturation magnetization and exchange and anisotropy constants. Their frequencies are therefore independent of the sample form. These modes are measured in our experiments and are shown by  $\bullet$  symbols in Fig. 10. The observed linear dependence of their frequencies on the mode number is related to predicted linear dispersion law of the Goldstone mode.<sup>2,3</sup>

In the Gilinskii mode both wall translations and oscillations transverse to the wall plane are simultaneously involved. Therefore it can be excited by rf fields which are either perpendicular or parallel to the wall plane. The frequency gap of Gilinskii mode  $\omega_G = \omega(k=0)$  for uniaxial ferromagnets is defined by the anisotropy parameter:  $\omega_G = \gamma 2K_u/M_s$ : it is usually very large compared to  $\omega_0$  of the Goldstone mode (appropriate frequencies are of the order of a few MHz for  $\omega_0$  and about 1 GHz for  $\omega_G$ ). The Gilinskii mode follows a nonlinear dispersion law with  $d^2\omega/dk^2 < 0$ .<sup>2,3,9</sup>

Additional branches of the wall excitation spectrum related to the wall structure can exist. In ferromagnets with cubic and small additional uniaxial anisotropy (e.g., in pure YIG)  $180^\circ$  walls consist of two subwalls of  $71^\circ$  and  $109^\circ$ . Breathing vibrations of a wall of this composition lead to a new branch of the spectrum. It is located at frequencies between the Goldstone mode and the Gilinskii mode.<sup>3</sup> The existence of a similar branch was predicted for a Néel wall.<sup>10</sup>

The above-mentioned theories of the domain wall excitation spectrum cannot be directly applied for the description of the present experiments and therefore we analyze the results qualitatively. In our case the walls have no subwalls and their structure, Eq. (19), is similar to that of simple Bloch walls in uniaxial ferromagnets. Therefore, breathing wall vibrations are unlikely to occur. In addition, the experiments show that wall resonances are effectively excited by rf

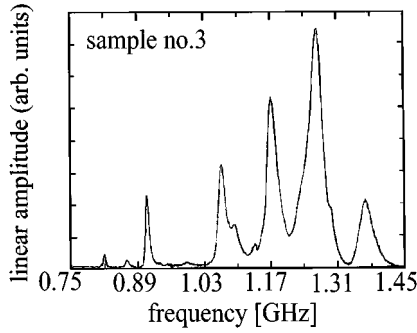


FIG. 11. Frequency response of a 180° domain wall in [100]-oriented  $\text{Lu}_{2.2}\text{Bi}_{0.8}\text{Fe}_5\text{O}_{12}$  film.

fields which are either parallel or perpendicular to the wall plane. Therefore the observed resonances are supposed to be related to the excitation of the Gilinskii mode or its analog for the material concerned. The observed nonlinear dependence of the appropriate resonance frequencies on the mode number (Fig. 9) qualitatively agrees with the predicted dispersion law of the Gilinskii mode.<sup>2,3,9</sup> An improved estimation of the frequency gap of the Gilinskii mode has recently been made for the case of a pure Bloch wall in bulk ferromagnet with cubic and uniaxial magnetic anisotropies:  $\omega_G = (2\gamma/M)[K_1(K_u - K_1)]^{1/2}$  (Ref. 11). It yields the value of  $\omega/2\pi = 310$  MHz for sample 2 in a qualitative agreement with the measured value 560 MHz. In sample 1 the domain walls are not of the Bloch-wall type, and therefore the above expression does not apply in this case.

#### IV. RESONANCES OF 90° AND 180° DOMAIN WALLS IN [100]-ORIENTED GARNET FILMS

Two different kinds of straight plane domain walls are observed in [100]-oriented samples: 180° walls parallel to the [011] and [011] directions and 90° walls parallel to the [010] and [001] directions. The domain wall thickness visible in a microscope is about 0.5 to 1  $\mu\text{m}$  and larger than that for [110]-oriented films: for 90° walls it is a little bit larger than for 180° walls. The calculated structure of 180° domain walls is formally described by Eq. (19) with  $q$  and  $\Delta$  replaced by  $q_1$  and  $\Delta_1$ :

$$q_1^2 = -\frac{K_1 + 4K_u}{2(K_1 - 2K_u)}, \quad \Delta_1^2 = \frac{2A}{K_1 - 2K_u}. \quad (21)$$

Expressions describing the structure of 90° walls are of the form:

$$\tan\psi = q_2 \sinh \frac{y}{\Delta_2}, \quad (22)$$

where parameters  $q_2$  and  $\Delta_2$  are given by

$$q_2^2 = \frac{2K_u}{2K_u - K_1}, \quad \Delta_2^2 = \frac{4A}{K_1 - 2K_u}. \quad (23)$$

Figure 11 shows the measured frequency response of 180°

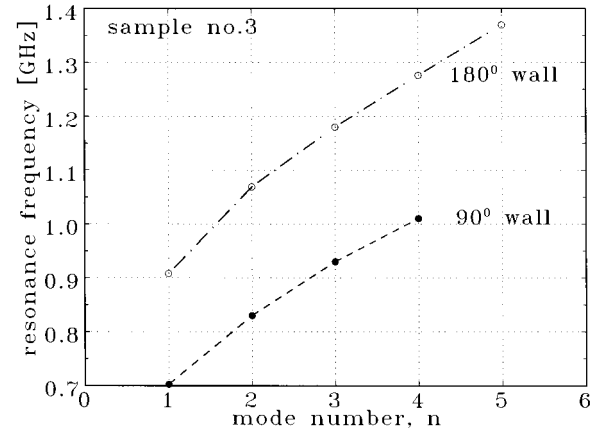


FIG. 12. Plot of resonance frequency vs mode number  $n$  for 180° and 90° domain walls in [100]-oriented films.

domain walls. All resonance modes seen in the top of the figure disappear when the wall is removed from the excitation region by a small dc induction ( $\sim 0.1$  mT). Only the FMR peak is observed in that case. The lowest domain wall resonance at the frequency of 0.91 GHz is characterized by a small linewidth of about 4.5 MHz like in the case of [110]-oriented films. Similar resonances are observed for 90° walls, but at lower frequencies. The dispersion of resonance frequency vs mode number for both 180° and 90° walls is shown in Fig. 12. A nonlinear dispersion law for both kinds of walls is revealed as is the case for [110] films. No influence of Bloch lines on all the above spectra is found.

For [100]-oriented films the estimation of the frequency gap of the Gilinskii mode of a 180° Bloch wall is  $\omega_G = (\gamma/M)[2K_1(2K_u - K_1)]^{1/2}$  (Ref. 11). It yields a frequency of 250 MHz for sample 3, the measured frequency is 910 MHz. The reason for this discrepancy is not yet known.

#### V. CONCLUSIONS

Low-anisotropy magnetic garnet films with in-plane magnetization are suitable materials for the investigation of a variety of branches of elementary and nonlinear excitations related to domains, domain walls, and Bloch lines. The present experiments show that in addition to the well-known low-frequency mode of domain wall translational (flexural) vibrations there exists a new higher-frequency mode with quite a different nonlinear dispersion law. These modes are promising for applications in integrated optics, e.g., for high-frequency light modulation.

#### ACKNOWLEDGMENTS

V.T.S. thanks Alexander von Humboldt Stiftung for support and hospitality during his stay in Germany. We thank Dr. S. Sure, M. Wallenhorst, and Professor W. Tolksdorf for the preparation of garnet films, Professor A. F. Popkov for fruitful discussions, and Dr. W. Bodenberger for helpful technical assistance. We also thank Deutsche Forschungsgemeinschaft, Sonderforschungsbereich 225, for financial support.

- <sup>1</sup>A. P. Malozemoff and J. C. Slonczewski, *Magnetic Domain Walls in Bubble Materials* (Academic, New York, 1979).
- <sup>2</sup>I. A. Gilinskii, Zh. Eksp. Teor. Fiz. **68**, 1032 (1975) [Sov. Phys. JETP **41**, 511 (1975)].
- <sup>3</sup>A. V. Mikhailov and I. A. Shimokhin, Phys. Rev. B **48**, 9569 (1993).
- <sup>4</sup>V. S. Gornakov, V. I. Nikitenko, I. A. Prudnikov, and V. T. Synogach, Phys. Rev. B **46**, 10 829 (1992).
- <sup>5</sup>V. S. Gornakov, V. I. Nikitenko, and V. T. Synogach, IEEE Trans. Magn. **29**, 2073 (1993).
- <sup>6</sup>B. Lührmann, H. Dötsch, and S. Sure, Appl. Phys. A **57**, 553 (1993).
- <sup>7</sup>A. Hubert, *Theorie der Domänenwände in Geordneten Medien* (Springer-Verlag, Berlin, 1974).
- <sup>8</sup>V. T. Synogach, Fiz. Tverd. Tela (Leningrad) **32**, 3475 (1990) [Sov. Phys. Solid State **32**, 2015 (1990)].
- <sup>9</sup>I. A. Shimokhin, Phys. Status Solidi B **167**, 243 (1991).
- <sup>10</sup>J. C. Slonczewski, J. Appl. Phys. **55**, 2536 (1984).
- <sup>11</sup>A. F. Popkov (unpublished).